

# Using Folded Proteins as Mechanically Well-Defined Units to Understand Fatigue Fracture in Hydrogels: Bridging Single Molecule and Bulk Studies

Liang Dong<sup>1,2,\*</sup>, Puyu Cao<sup>3,\*</sup>, Huiyan Chen,<sup>2</sup> Yu Zhang<sup>2</sup>, Ying Li,<sup>4</sup> Bin Chen,<sup>3,†</sup> Yi Cao<sup>2,5,6,‡</sup> and Hai Lei<sup>1,§</sup>

<sup>1</sup>*School of Physics and Institute for Advanced Study in Physics, Zhejiang University, Hangzhou 310027, China*

<sup>2</sup>*National Laboratory of Solid State Microstructures, School of Chemistry, Nanjing University, Nanjing 210093, China*

<sup>3</sup>*Department of Engineering Mechanics, Zhejiang University, Hangzhou 310027, China*

<sup>4</sup>*Institute of Advanced Materials and Flexible Electronics (IAMFE), School of Chemistry and Materials Science, Nanjing University of Information Science and Technology, Nanjing, 210044, China*

<sup>5</sup>*Chemistry and Biomedicine Innovation Center (ChemBIC), Nanjing University, Nanjing 210093, China*

<sup>6</sup>*MOE Key Laboratory of High Performance Polymer Materials and Technology, Nanjing University, Nanjing 210093, China*



(Received 12 August 2025; accepted 3 April 2026; published 11 May 2026)

Hydrogels are widely used in applications that require durability under cyclic loading, yet fatigue fracture often limits their reliability. The underlying physical principles of hydrogel fatigue remain elusive due to the complex interplay between molecular-scale events and macroscopic crack propagation. Here, we harness folded protein domains as reversible, mechanically defined sacrificial units within polyprotein crosslinkers to directly correlate single-molecule unfolding with bulk fatigue behavior. By engineering hydrogels with protein domains that have tunable unfolding forces (100–1500 pN) and varying the number of domains per crosslink, we demonstrate that random networks incorporating weaker protein domains can achieve unexpectedly high fatigue thresholds through distributed energy dissipation. Moreover, we develop a force response model—introducing a generalized force-decay law and integrating unfolding or refolding kinetics—to establish a quantitative framework for understanding fatigue behavior. This combined approach offers a versatile strategy for designing next-generation, fatigue-resistant hydrogels that retain low stiffness and high extensibility.

DOI: [10.1103/bcq4-xw5q](https://doi.org/10.1103/bcq4-xw5q)

Subject Areas: Biological Physics, Materials Science, Soft Matter

## I. INTRODUCTION

Hydrogels are increasingly used in applications that demand durability under cyclic loading [1,2], from artificial cartilage to soft robotics [3], yet they are notoriously prone to fatigue fracture. Fatigue fracture in hydrogels—the gradual growth of cracks under repeated subcritical loads—poses a critical challenge for the reliability of these soft materials [4,5]. A fundamental difficulty has been reconciling experimental observations of hydrogel fracture with classical theories. Traditional models (e.g., the

Lake-Thomas theory [6]), which estimates fracture energy based on rupture of a single layer of bridging strands [Fig. 1(a)], significantly underestimate the energy dissipation observed during crack propagation [7]. This discrepancy suggests that real networks dissipate far more energy during crack propagation than simple theory predicts, highlighting the need for improved frameworks. Recent theoretical advances by Zhao and co-workers introduced nonlocal dissipation concepts [7,8], where crack-induced bond breaking extends into a broader region of the network, partially closing the gap between theory and experiment [Fig. 1(b)]. Craig and colleagues further modified this theoretical model, considering a nonlinear dependence of stored energy of polymer strands [9]. This model provided a satisfactory explanation for the energy dissipation of network with mixed strong and weak bonds and underscored the intricate interplay between network topology and molecular bond rupture events [10]. Despite these efforts, fully quantitative agreement between theory and experiment remains elusive, largely due to the multiscale nature of bond breaking in tough hydrogels.

\*These authors contributed equally to this work.

†Contact author: [chenb6@zju.edu.cn](mailto:chenb6@zju.edu.cn)

‡Contact author: [caoyi@nju.edu.cn](mailto:caoyi@nju.edu.cn)

§Contact author: [leihai@zju.edu.cn](mailto:leihai@zju.edu.cn)

Published by the American Physical Society under the terms of the [Creative Commons Attribution 4.0 International license](https://creativecommons.org/licenses/by/4.0/). Further distribution of this work must maintain attribution to the author(s) and the published article's title, journal citation, and DOI.

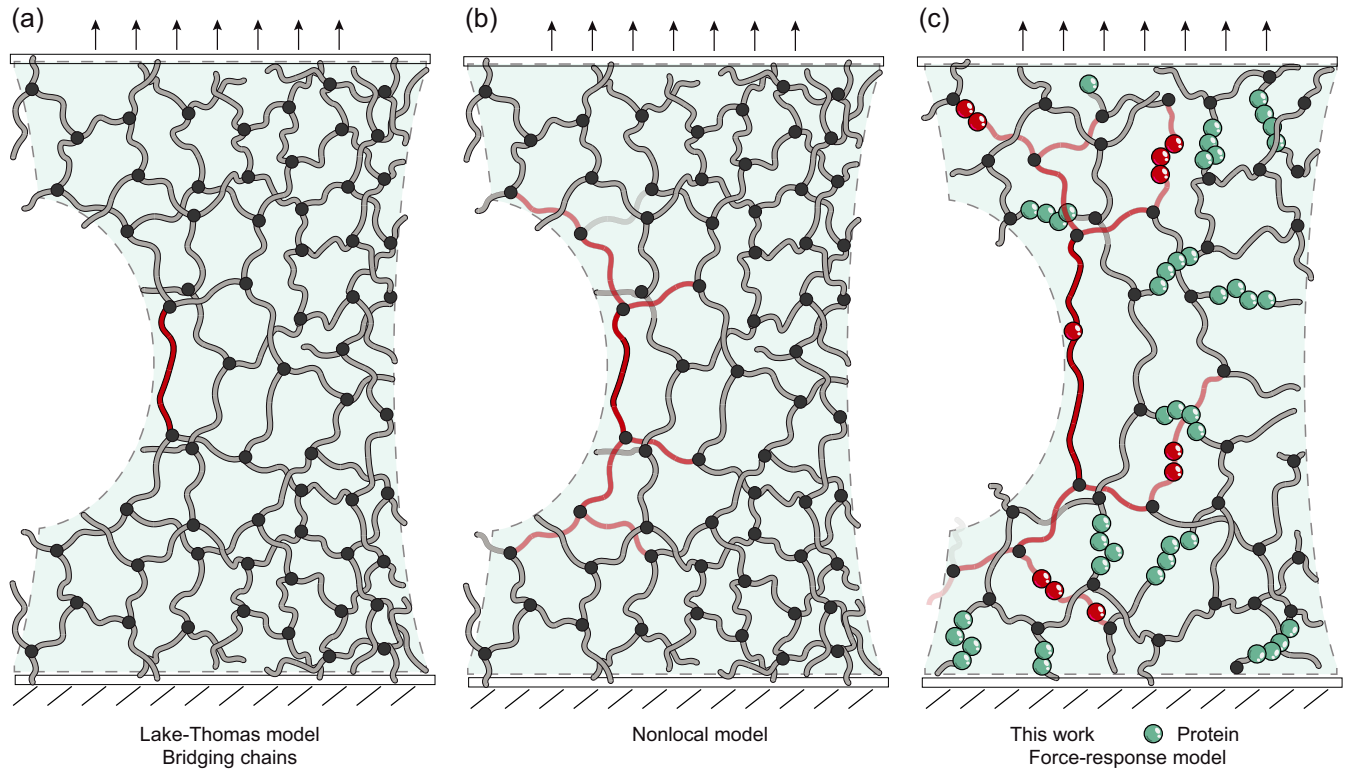


FIG. 1. Conceptual scheme of energy dissipation during crack propagation. (a) In the Lake-Thomas model, the intrinsic fracture energy equals the energy needed to break a single layer of polymer chains. (b) The intrinsic fracture energy mainly results from nonlocal energy dissipation by relaxing polymer chains far away from the crack tip. (c) In our force-response model, we suggest that force transduction at the crack tip through the polymer network couples with the conformational change of the polymer leading to an expanded crack zone. In our case the conformational change of polymer involves force-dependent protein unfolding or folding.

Mechanophores—force-sensitive covalent crosslinkers—have emerged as a powerful tool to probe and control such mechanisms in hydrogels [11]. By incorporating mechanophores of tunable reactivity into polymer networks, researchers have revealed many interesting interplays between network structure and bond strength for fatigue resistance [12–14]. However, mechanophores face inherent constraints: because mechanophores signal energy dissipation through irreversible bond rupture, their activation can deplete network integrity over time [13–16]. In addition, if their activation force is too high relative to the surrounding polymer chains, nonspecific backbone scission may occur, complicating the correlation between crosslinker strength and fracture energy [11,17]. These challenges motivate the search for alternative strategies.

In this work, we introduce folded proteins as reversible, mechanically defined sacrificial units within the polymer network and suggest a “force-response model” to couple force-induced conformational change of polymer at the molecular level to the crack propagation at the macroscopic level [Fig. 1(c)]. Unlike small-molecule mechanophores, folded protein domains can be engineered to unfold at predetermined forces and can be concatenated to enable multiple unfolding events per crosslink [18]. Unfolding does not break the polymer backbone; rather, it extends the

protein segment while preserving network connectivity. By incorporating protein domains with unfolding forces spanning 100–1500 pN and varying the number of domains per crosslink (from 1 to 16), we establish a model system to directly correlate protein unfolding or folding events with macroscopic fatigue crack growth resistance. This approach overcomes the one-time, irreversible nature of mechanophore activation and offers a pathway for designing fatigue-resistant hydrogels without increasing stiffness.

## II. RESULTS

### A. Hydrogel design

Our strategy is to incorporate custom-designed polyprotein crosslinkers into a hydrogel network, thereby using folded protein domains as the sacrificial segments that can unfold under stress. The network structure of the hydrogels is depicted in [Fig. 2(a)], which is made of polyprotein crosslinked random polymer network [18]. Each polyprotein consists of one or multiple identical globular domains connected in tandem. These protein domains were chosen based on their known single-molecule unfolding forces as measured by atomic force microscopy (AFM)-based single molecule force spectroscopy (SMFS) [19] to serve as

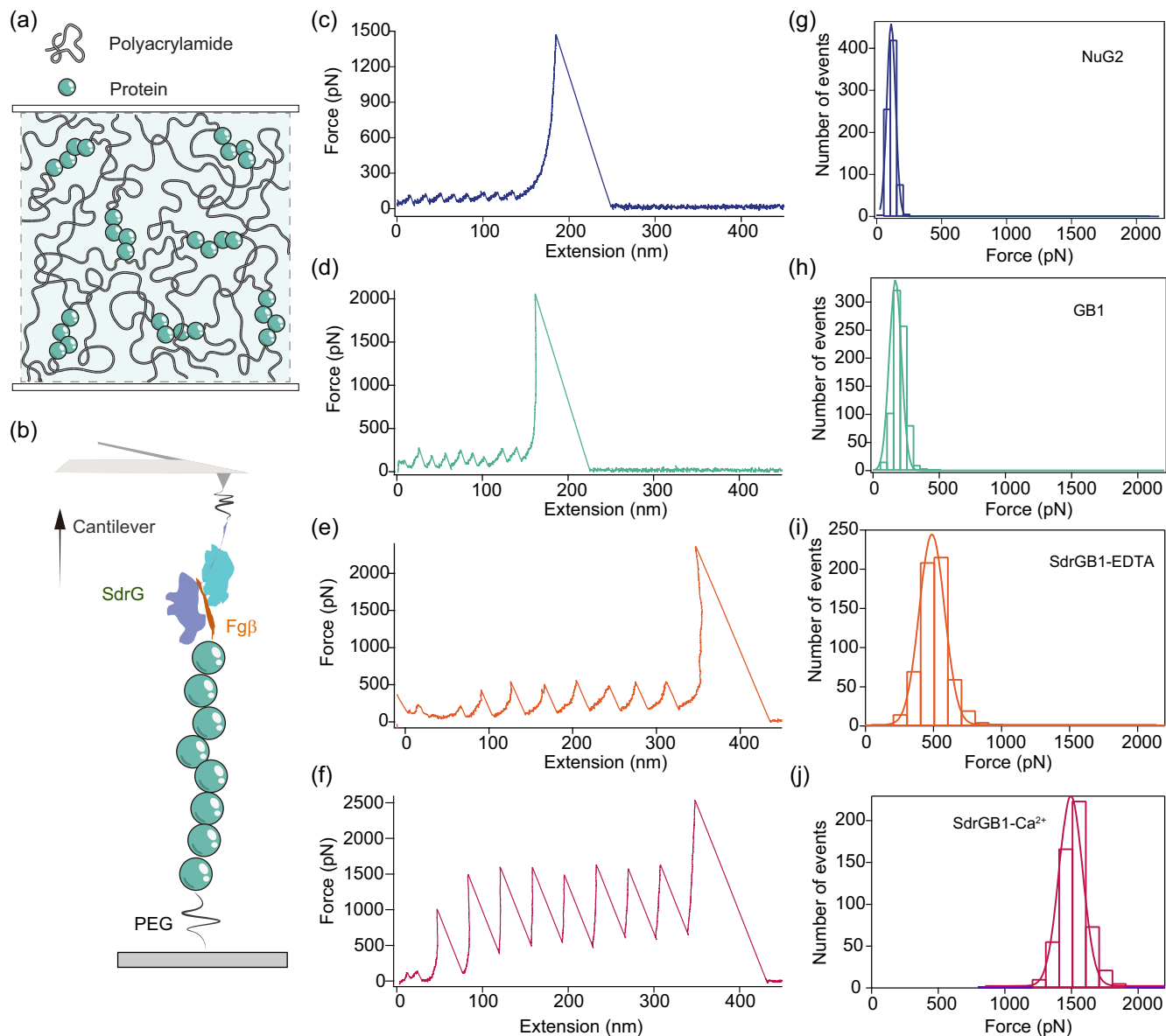


FIG. 2. Design principle for the antifatigue hydrogels and molecular mechanics characterization. (a), Schematic illustration of the hydrogel, in which the polyprotein as crosslinkers and polyacrylamide as the percolating phase to form random polymer network. (b) Schematic of the AFM based single molecule force spectroscopy experiments. (c)–(f) Representative single molecule force-extension curves of  $(\text{NuG2})_8$ ,  $(\text{GB1})_8$ , and  $(\text{SdrGB1})_8$  with EDTA and  $\text{Ca}^{2+}$ , respectively. (g)–(j) The histograms of unfolding force of NuG2, GB1, SdrGB1-EDTA, and SdrGB1- $\text{Ca}^{2+}$ , respectively. By fitting with Gaussian fit, the unfolding forces are  $112.6 \pm 47.2$  pN (mean  $\pm$  S.D.) for NuG2 ( $n = 758$ ),  $193.3 \pm 64.8$  pN for GB1 ( $n = 794$ ),  $474.6 \pm 131.6$  pN for SdrGB1 with EDTA ( $n = 601$ ), and  $1492.7 \pm 130.5$  pN for SdrGB1 with  $\text{Ca}^{2+}$  ( $n = 565$ ), respectively.  $n$  is the total number of events.

molecular force gauges within the network. Specifically, three distinct protein domains we used are NuG2 [20], GB1 [21], and SdrGB1 [22], as they are known in the literature for their diverse mechanical properties. Additionally, the mechanical stability of SdrGB1 can be adjusted through binding with calcium ions [22]. Consequently, these polyprotein crosslinkers offered us the means to investigate how the number of protein domains and their associated mechanical stabilities impact the fatigue resistance of the hydrogels.

## B. Mechanical properties of the polyprotein crosslinkers

While the mechanical stability of GB1, NuG2, and SdrGB1 has been previously explored using various protein constructs, we sought to mitigate potential biases arising from different experimental designs. To achieve this, we assessed the mechanical stabilities of these protein domains, each with eight tandem repeats and well-defined pulling geometry using AFM-based single molecule force spectroscopy [23] [Fig. 2(b) and see Appendix for details].

These polyproteins were stretched in Tris buffer (10 mM Tris with 100 mM NaCl at pH 7.4) at a constant pulling speed of  $1000 \text{ nm s}^{-1}$ . Mechanical unfolding of these polyproteins yielded characteristic sawtoothlike force-extension curves [Figs. 2(c)–2(f)], with each peak corresponding to the unfolding of an individual domain. The final peak, exceeding 2 nN, resulted from the break of the polyproteins from the tether. Specifically, the unfolding forces were approximately 110 pN for NuG2 [Fig. 2(g)], 200 pN for GB1 [Fig. 2(f)], 500 pN or 1.5 nN for SdrGB1 in the absence or presence of  $\text{Ca}^{2+}$ , respectively. The kinetic parameters underlying the unfolding of these protein domains were determined using the Dudko-Szabo-Hummer model [24] and the results are summarized in the Supplemental Material [25]. These distinctive mechanical stabilities among the protein domains imply that polyproteins with these domains possess varying abilities to dissipate mechanical load at the molecular level.

### C. Hydrogel preparation and mechanical test

We prepared hydrogels with identical polymer network structures (same polymer molecular weight, same crosslink density) differing only in the protein crosslinker composition. Specifically, we designed twelve types of polyprotein crosslinkers, denoted as  $(\text{GB1})_2$ ,  $(\text{GB1})_4$ ,  $(\text{GB1})_8$ ,  $(\text{GB1})_{16}$ ,  $(\text{NuG2})_2$ ,  $(\text{NuG2})_4$ ,  $(\text{NuG2})_8$ ,  $(\text{NuG2})_{16}$ ,  $(\text{SdrGB1})_1$ ,  $(\text{SdrGB1})_2$ ,  $(\text{SdrGB1})_4$  and  $(\text{SdrGB1})_8$  (see details in the Supplemental Material [25]). Notably, GB1 and NuG2 possess an equal number of amino acids, while SdrGB1 is approximately twice the size of GB1 and NuG2 (see details in the Supplemental Material [25]). In addition, for SdrGB1 polyprotein crosslinked hydrogels, we can simply add or remove  $\text{Ca}^{2+}$  to control the mechanical properties of the crosslinkers without changing the network structure. Thus, we have four series of hydrogels (16 types) with crosslinkers of varied mechanical strength.

Our hydrogels were fabricated using polyacrylamide as the percolating phase and the polyprotein as the crosslinker, employing SNAP-BG chemistry to integrate the antifatigue network [18], as previously published; see Appendix for details.

We first conducted tensile tests on all 16 hydrogel variants to examine their mechanical properties. All mechanical assessments were carried out at room temperature, in ambient air, using a mechanical testing machine equipped with a 10-N load cell [Figs. 3(a) and 3(b)]. Unless specified otherwise, the rate of stretch was maintained at a constant  $10 \text{ mm min}^{-1}$ . The stress-strain curves for both unnotched and notched samples of all 16 hydrogel types under tension are depicted in Figs. 3(c)–3(f). As the number of protein domains increased, there was a slight rise in modulus, likely due to the higher weight percent of the crosslinker in the hydrogels. Nevertheless, all 16 hydrogels, despite the varying number of protein domains, exhibited a

similar Young's modulus, approximately 9 kPa [Fig. 3(g)]. Furthermore, when these hydrogels were stretched to a strain below the point of fracture and then relaxed, the forward and reverse stress-strain curves closely overlapped (see details in the Supplemental Material [25]). These observations indicate that the small-strain elastic response is dominated by the percolating polymer network, while the folded polyprotein domains behave as mechanically rigid crosslinkers under homogeneous deformation. However, the unfolding of the polyprotein crosslinkers did contribute to the maximum stress and strain. Because of their distinct energy dissipation capabilities, the hydrogels displayed varying fracture stress and strain. Generally, as the number of protein domains increased, the fracture stress and strain also increased for all four sets of hydrogels. However, the fracture stress and strain did not follow the trend of the unfolding forces of all the domains, indicating complex energy dissipation mechanisms during hydrogel fracture.

Fatigue fracture tests were performed on notched hydrogel samples under cyclic loading at a fixed frequency of 1 Hz, unless otherwise specified [4]. We applied a cyclic loading regime at a fixed peak stress (or strain) that is a fraction of the gel's nominal failure stress, and monitored crack growth per cycle. The primary metric for fatigue resistance is the fatigue threshold, usually defined as the maximum energy release rate (or strain energy intensity) under which a crack does not grow (or grows negligibly slowly) per cycle. Practically, we determine the threshold by finding the lowest cyclic load amplitude at which steady crack propagation occurs. We compare this threshold (or equivalently, the critical energy release rate  $G_c$ ) across different hydrogel formulations to assess the impact of the protein units (Fig. 4 and see details in the Supplemental Material [25]). For all four sets of hydrogels, the fatigue thresholds consistently increased with the number of protein domains, denoted as  $n$ . Recalling that the size of SdrGB1 is twice that of GB1 and NuG2, the length of the unfolded crosslinkers of polyproteins made of SdrGB1 matches that of GB1 and NuG2 with twice the number of repeats. Upon comparing crosslinkers of equal length, we observed that the fatigue thresholds showed a nonlinear relationship with the unfolding forces of the protein domains. This finding is counterintuitive, as one might assume that a higher unfolding force (meaning the sacrificial unit can sustain more tension before yielding) would protect the network better. This finding also agrees with recent finding that networks with some weak strands outperform those with exclusively strong strands [10]. Notably, the enhancement in fatigue resistance does not require extensive unfolding throughout the bulk material. Instead, energy dissipation is expected to be highly localized in regions of concentrated stress near the crack tip, enabling an increased fatigue threshold without incurring a stiffness-toughness trade-off.

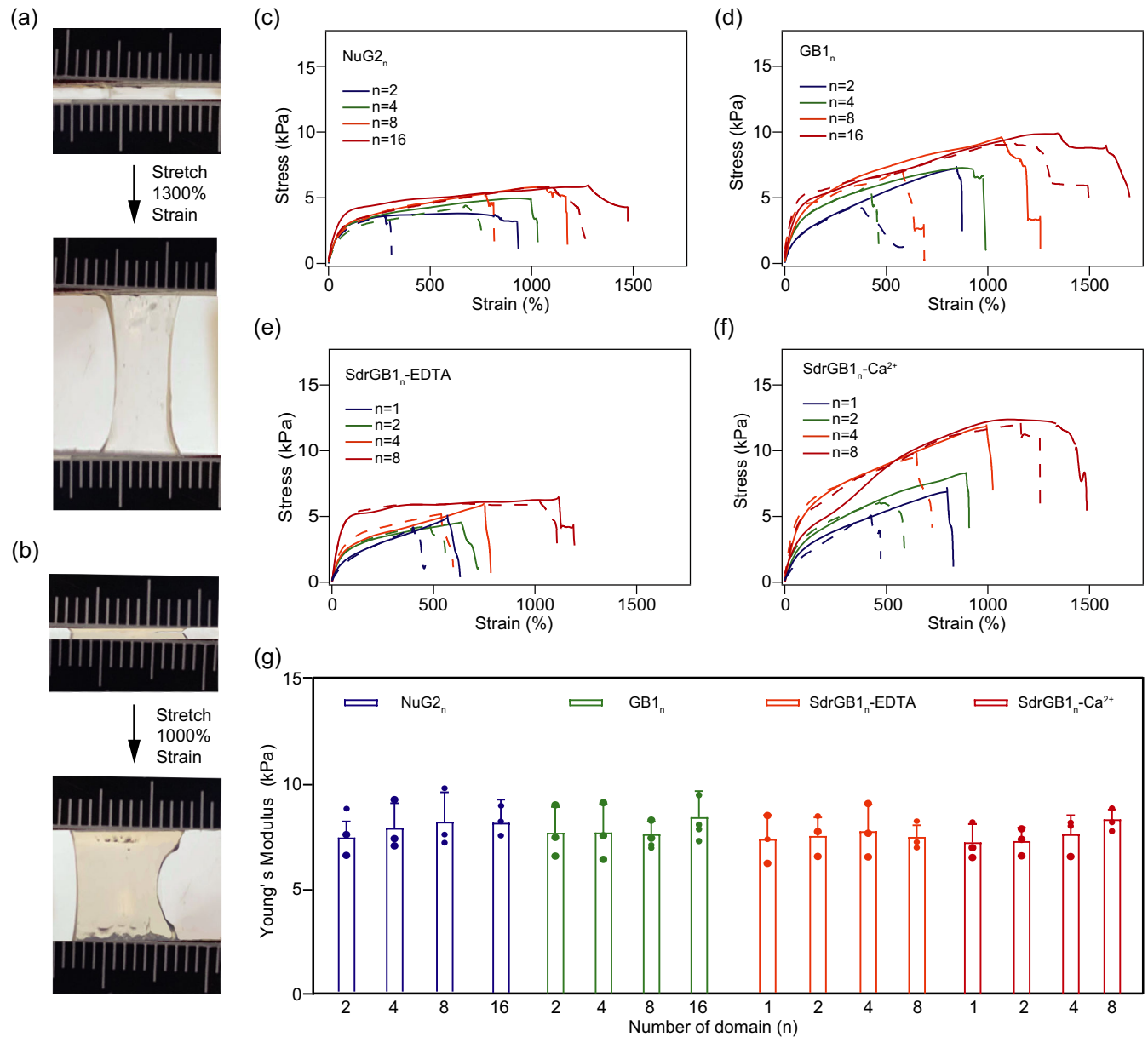


FIG. 3. Mechanical characterization of hydrogels. (a) Tensile test of the unnotched hydrogel. The hydrogel was stretched to 13 times of its initial length. (b) The notched hydrogel was stretched to 10 times its initial length without fracture. (c)–(f) Stress-strain curves for unnotched (solid line) or notched (dotted line) samples with polyproteins as crosslinkers, including NuG<sub>2n</sub> (c), GB1<sub>n</sub> (d), SdrGB1<sub>n</sub> with EDTA (e), and Ca<sup>2+</sup> (f), respectively,  $n$  is the domain number of the polyproteins. (g) Young's modulus of all 16 gels.

#### D. Theoretical model

To interpret these experimental results, we developed a theoretical model building on multi bond fracture framework [7,8], which employs a hierarchical Cayley tree structure to represent the hydrogel network, where force decays exponentially across generations of strands—a feature critical for predicting fatigue thresholds in networks. The model was subsequent advanced by Craig and collaborators by integrating the nonlinear elasticity of stretched polymer chains, enabling predictions of fracture

behavior in networks with mechanically heterogeneous crosslinkers [9]. However, these prior nonlocal models with hierarchical treelike networks oversimplified the system by assuming homogeneous chain behavior and uniformly folded domains. Here, we extended this model to a new force-response model [Fig. 5(a)] that directly couples force redistribution with the kinetic unfolding or refolding of folded domains, resolving limitations in existing frameworks (See Supplemental Material [25] for details).

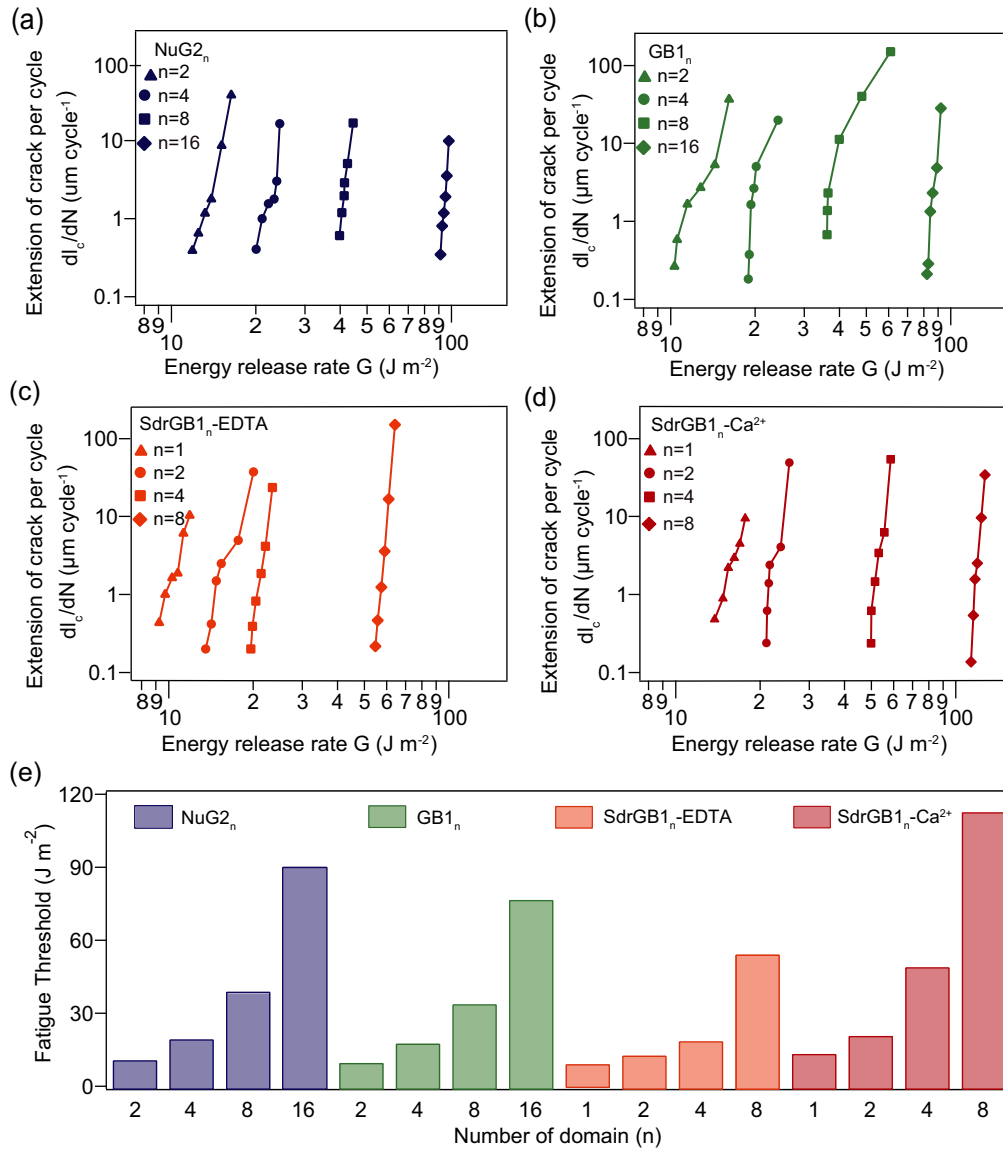


FIG. 4. Fatigue fracture properties of the hydrogels. (a)–(d) Extension of crack per cycle as a function of the energy release rate of all 16 gels. (e) The fatigue thresholds of all 16 gels.

First, we employed a singular force decay across layers together with layer-dependent chain number, given by

$$F_i = F_1 \cdot i^s, \quad m_i = i^{-s} \quad (1)$$

aligning with crack-tip stress singularity principles [26,27], where the force and the chain number in the  $i$ th layer are denoted as  $F_i$  and  $m_i$ , respectively, with  $F_1$  being the chain force in the first layer, and  $s$  is a free parameter reflecting the spatial decay of force distributions. We noticed that previous approaches adopted the oversimplified exponential force decay [ $F_i = F_1 \cdot (f_n - 1)^{-(i-1)}$ ], where  $f_n$  is the functionality of the crosslinks and would be equal to 3 in our case, in which they assumed that force on one strand is equally distributed to the strands of its lower generation. However, considering force is a vector [Fig. 5(a)], as far as

one strand at the crosslink reaches mechanical balance, the amplitude of its force can vary between 1 to  $1/(f_n - 1)$ . Instead, we employed the singular force decay across layers in our model to capture crack-tip stress singularity, where  $s$  depends on the network topology and connectivity of the hydrogels. Note that  $s$  should depend on the network topology and connectivity of the hydrogels.

Second, we incorporated the force-response unfolding or refolding kinetics of folded domains based on Bell's theory [28]. One crucial aspect for fatigue in our gels is the time and cycle dependence of energy dissipation of a sacrificial bond. Under cyclic loading, a sacrificial bond might not break on the first loading; however, repeated loading can cause bond breakage via accumulated damage or probabilistic failure (a kind of “fatigue” on the molecular scale) and the reformation of the bond due to the refolding

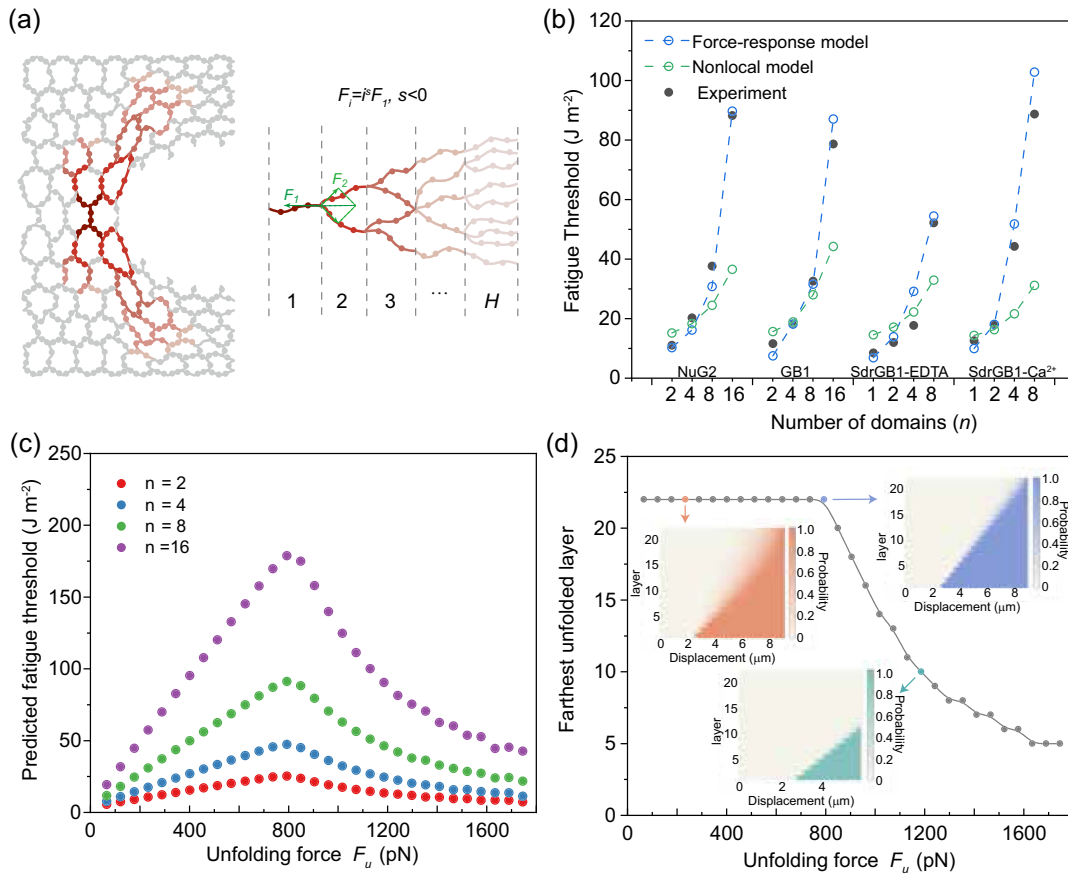


FIG. 5. Model prediction. (a) Schematic illustration of a fractured polymer chain along the crack path, deformed neighboring chains, and the force-response model with singular force decay across layers. (b) Comparison of fatigue thresholds among experiments, the prediction by the previous nonlocal model and the current force-response model of fabricated hydrogels with folded domains of GB1, NuG2, SdrGB1-EDTA, or SdrGB1- $\text{Ca}^{2+}$ , when the number of folded domains varies within a single polymer chain. (c) The predicted fatigue threshold increases and then decreases with the unfolding force. (d) Predicted protein unfolding probability occurs away from the bridging strand for hydrogels with 16 domains in a polymer chain. The generation of farthest unfolded layers is governed by the force-dependent unfolding and folding kinetics of folded domains. For simplicity, we estimate the effect of unfolding force on the maximum extent of the unfolding zone by modifying the unfolding rate while fixing the folding rate (750/s) (see details in the Supplemental Material [25]). Below a threshold force, the unfolding zone can extend up to 23 layers, corresponding to a displacement of  $\sim 8.5 \mu\text{m}$ . However, increasing the unfolding force beyond this threshold reduces the extent of the unfolding zone. Insets show the predicted displacement and the corresponding unfolding probability at distinct layers for three representative unfolding forces.

of protein domains as well (a kind of “healing” on the molecular scale). In essence, even if the peak force on a protein domain is slightly below its nominal single-cycle unfolding force, there is a finite probability that thermal fluctuations during the load dwell could trigger unfolding. Repeated cycles increase this probability. With Bell’s law [28], the unfolding and refolding rate of domains in the  $i$ th layer,  $k_{uf,i}$  and  $k_{f,i}$  are given by

$$k_{uf,i} = k_{uf}^0 \exp\left(\frac{F_i z_{uf}}{kT}\right) \quad \text{and} \quad k_{f,i} = k_f^0 \exp\left(\frac{-F_i z_f}{kT}\right), \quad (2)$$

where  $k_{uf}^0$  and  $k_f^0$  are the unfolding rate and the refolding rate when the chain force is zero, respectively, and  $z_{uf}$  and  $z_f$  are the respective transition distance, which are

measured in single-molecule experiments and vary for different types of protein domains,  $T$  is the absolute temperature and  $k$  is the Boltzmann constant.

To compute the fatigue threshold, we numerically simulated a loading cycle by imposing a constant stretching velocity on the hierarchical structure and discretizing the loading cycle into small time steps. At each step, the global stretch was prescribed and the layer forces  $F_i$  are solved by enforcing the constraint that the sum of the individual layer extensions equaled the imposed total stretch, together with the force-extension relations of the chains in each layer. Given  $F_i(t)$ , the unfolding and refolding rates were evaluated using Eq. (2), and the fraction of unfolded domains in each layer were advanced in time using explicit time integration. The effective contour length (and hence the force-extension response) of each layer was updated accordingly and carried into the next time step. The energy

dissipated in each layer over a loading cycle was then obtained by integrating the corresponding force-extension hysteresis loop. The total energy consumed within the  $i$ th layer when  $F_1$  approaches the bond breaking force,  $F_c$ , would be given by  $U_i = m_i \int F_i dx_i$ , and the total energy  $U$  consumed within the tree (total layers  $H$ ) would be

$$U = U_1 + 2 \sum_{i=2}^H U_i, \quad (3)$$

where  $x_i$  denotes the extension of chains in the  $i$ th layer, and the factor of 2 accounts for the structural symmetry of the tree.

Then, following the Lake-Thomas theory [6], the fatigue threshold based on our force-response model would be calculated by

$$\Gamma = \alpha N_{\text{chain}} U \lambda_S L_0, \quad (4)$$

where  $\alpha$  is a prefactor,  $\lambda_S$  is the free-swelling stretch of fabricated hydrogels,  $L_0$  is the initial length of the polymer chain,  $N_{\text{chain}}$  is the chain density of fabricated hydrogels at the free-swelling state, derived through Young's modulus  $E$  extracted from the force-stretch curve in experiments through  $E = 2(1 + \nu) N_{\text{chain}} k T \lambda_S^2$ , where  $\nu$  is Poisson's ratio.

To mimic experimental loading conditions with a loading frequency of 1 Hz, the simulations of fatigue thresholds of our hydrogels were conducted by imposing a constant stretching velocity to the farthest layer, enabling  $F_1$  reaches  $F_c$  within half a second. The parameters used in the simulation are provided in the Supplemental Material [25]. The model predictions of fatigue threshold are shown in Fig. 5(b), which demonstrates that the current model predictions better match experimental observations, particularly in capturing the influence of domain unfolding or refolding kinetics and the number of domains on fatigue thresholds. To further assess the robustness of the force-response model beyond a single theoretical construction, we implemented an independent coarse-grained polymer-network simulation that explicitly resolves crack-tip stress redistribution and unfolding or refolding kinetics; the two approaches show quantitative consistency in predicting fatigue thresholds (see details in the Supplemental Material [25]). Notably, increasing the number of domains substantially enhances the fatigue threshold by increasing energy dissipation upon loading. The model captures the nonlinear accumulation of damage: minor unfolding of weak protein domains which then significantly extends the life of the sample by reducing subsequent driving force—a behavior the initial theoretical formulation qualitatively suggested but did not explicitly calculate [7]. To assess the role of loading rate beyond the experimentally tested conditions, we systematically varied the loading frequency within the model, enabling an examination of how rate-

dependent bond kinetics modulated fatigue behavior (see details in the Supplemental Material [25]).

Furthermore, the fitted singular exponent  $s$  is close to  $-1/2$ , tentatively pointing to a near-linear stress-strain relationship in hydrogels [29,30]. By letting  $s$  be  $-1/2$ , we further adjusted the domain's unfolding force,  $F_u$ , by virtually modifying the unfolding rate,  $k_{uf}^0$ , of GB1 while keeping the folding rate constant at  $750 \text{ s}^{-1}$ , and then predicted its influence on the fatigue threshold. As shown in [Fig. 5(c)], the predicted fatigue threshold generally increases and then decreases with  $F_u$  and there exists a peak fatigue threshold with the corresponding unfolding force, denoted by  $F_u^m$ . In our simulation, when  $F_u < F_u^m$ , a higher unfolding force would result in more energy consumption, leading to higher predicted fatigue thresholds; When  $F_u > F_u^m$ , the total number of unfolded domains within the tree gradually decreases with the unfolding force, as shown in [Fig. 5(d)], which finally leads to a reduction in the predicted fatigue threshold. As also shown in [Fig. 5(c)], increasing the number of protein domains within a single polymer chain would generally increase the fatigue threshold.

One outcome of our refined model is a more general law for force decay across strand generations. In prior framework [7], one might assume an exponential decay in the force carried by successive layers of network strands as one moves away from the crack tip. Our results suggest that this decay can follow a singular pattern, closely resembling the stress singularity at a crack tip, which is tied to the force dependent protein folding or unfolding. In a network sense, the first-generation strands at the crack tip carry the highest force and break first; the second-generation strands (those that will become the new primary load-carriers after the first generation failed or unfolded) carry less force, and so on. Our model characterizes the force redistribution by replacing the assumption of uniform protein unfolding with a more realistic cascade of multistep kinetic events. Force-activated mechanochemical reactions can proceed in complex ways, influenced by the force distribution across different network generations and the activation forces at given loading rates. In our case, a highly expanded unfolding zone is observed only when the unfolding force is below 800 pN. Recent studies by Craig and colleagues also suggested that weakly crosslinked polymer networks can exhibit greater mechanical stability [31]—an observation that can be well explained by our model. We find that using this more general force-decay formula in the nonlocal fracture energy model yields improved agreement with experimental fracture energy values across different materials. In fact, the model aligns with the recent proposal by Hartquist *et al.* of a universal scaling law for intrinsic fracture energy in networks [10], while also explaining where that universality breaks down (i.e., when kinetics come into play). By refining the theoretical framework in this way, we bridge the gap between molecular-scale events

(protein unfolding or refolding under force) and macroscale consequences (hydrogel fatigue crack growth).

### III. DISCUSSION

These results demonstrate that embedding protein domains as mechanically defined sacrificial units provides an effective route to enhancing fatigue resistance without relying on pervasive bond exchange or large network rearrangement. Unlike conventional polymer networks, in which dissipation is typically coupled to irreversible bond breaking or viscoelastic relaxation, the present network architecture introduces spatially and temporally localized energy dissipation through force-activated protein unfolding. As a result, the network can dynamically redistribute stress under nonuniform deformation while preserving its bulk elastic integrity. This mechanism enables programmable control of fatigue behavior through the molecular parameters of the protein domains, including unfolding force, contour-length increment, refolding rate, etc. An illustrative example is provided in the Supplemental Material [25], where such force-activated dissipation promotes deformation homogenization in a heterogeneous cellular lattice under loading.

Importantly, our theoretical framework does not assume that protein domains fully unfold or refold within each loading cycle. Instead, unfolding and refolding kinetics are explicitly integrated during both loading and unloading using the Bell's model, allowing residual unfolded fractions to persist across cycles. This treatment captures the intrinsically nonequilibrium and history-dependent nature of the dissipation process. Within this framework, variations in loading frequency primarily modulate the magnitude of the fatigue threshold by altering the unfolding force and the extent to which force-activated domains are engaged during cyclic deformation, rather than changing the underlying dissipation mechanism itself (see details in the Supplemental Material [25]).

Our results are consistent with the universal scaling relation proposed for fatigue resistance in soft networks [32] within the regime where sacrificial elements can be effectively activated in the process zone. In protein-based hydrogels, the relevant dissipation length scale emerges from the collective unfolding of multiple protein domains near stress concentrators, rather than from a single chain-scission event. However, when the unfolding force of the protein domains becomes too large, these domains are no longer efficiently activated prior to macroscopic failure, leading to a reduction in the effective dissipation zone and a systematic deviation from the ideal scaling behavior. This highlights that the applicability of universal fatigue scaling laws depends critically on the force- and kinetics-dependent accessibility of molecular dissipation mechanisms (see Supplemental Material [25]).

More broadly, this framework generalizes previously used truss-lattice or binary force-decay models by introducing a

parameterized description of force-activated dissipation that directly incorporates molecular force thresholds and kinetic rates. Whereas earlier models [9,33] often assume uniform or stepwise force decay along load paths, the present approach allows dissipation to be distributed adaptively according to the underlying molecular response. In this sense, the framework is not limited to protein unfolding and may, in principle, be extended to other classes of sacrificial interactions [34], such as hydrophobic associations or dynamic metal-ligand coordination, provided their force-dependent kinetics are known.

Another significant insight concerns the role of bond strength heterogeneity. We show that networks incorporating weaker protein domains can exhibit larger process zones and higher fatigue thresholds than those with stronger protein domains—an observation paralleling recent mechanophore-based studies [13]. In practice, a network with a population of sacrificial bonds or folded protein domains that yield readily distributes deformation over a larger volume, reducing stress concentration at the crack tip. This principle, also observed in double-network and mechanophore-linked hydrogels, underscores the importance of designing for damage delocalization to enhance toughness and fatigue resistance [35].

Beyond the qualitative notion that “weaker can be better,” our results reveal a nonmonotonic dependence of fatigue resistance on the unfolding force of sacrificial domains [Fig. 5(c)]. If the unfolding force is too small, domains are activated even under moderate loading, leading to premature exhaustion of folded domains and low dissipation capacity, which ultimately promotes brittle failure. Conversely, if the unfolding force is too large, domains remain inactive until near macroscopic fracture, preventing effective stress redistribution and again limiting fatigue resistance. Optimal performance therefore arises within an intermediate force window, where sacrificial domains are selectively activated in regions of high stress concentration. This establishes a rational design principle in which unfolding force, refolding kinetics, and network connectivity jointly determine fatigue performance, enabling predictive rather than trial-and-error tuning of soft materials.

Overall, our work bridges mechanochemical approaches and biomolecular engineering. By employing whole protein domains as precise, tunable mechanochemical units, we not only confirm the principles of force-sensitive bond toughening but also provide a general, quantitative framework for designing next-generation, fatigue-resistant hydrogels. It is important to note, however, that extremely weak proteins may unfold during gel swelling, which could complicate data interpretation. Notably, while previous strategies—such as hierarchical designs [36–38] or dynamic bonds [39–41]—improve fatigue resistance, they often increase stiffness [36,42], which is undesirable for applications requiring high extensibility and low

compliance. In contrast, our method enhances the fatigue threshold without compromising softness, thereby broadening the design toolbox for antifatigue hydrogels.

### ACKNOWLEDGMENTS

This work was supported by the National Natural Science Foundation of China (Grants No. T2222019, No. T2225016, No. 12574234, and No. 12372318), and Zhejiang Provincial Natural Science Foundation of China (Grant No. LZ23A020004).

### DATA AVAILABILITY

The data that support the findings of this article are openly available [25].

## APPENDIX: MATERIALS AND METHODS

### 1. Protein engineering

Genes encoding  $Fg\beta-(GB1)_8-Cys$ ,  $Fg\beta-(NuG2)_8-Cys$ ,  $Fg\beta-(SdrGB1)_8-Cys$  and  $SdrG-Cys$  were cloned into pQE80L vectors using standard molecular biology techniques. These proteins were expressed in *Escherichia Coli* (GenScript, China), purified by  $Co^{2+}$  affinity chromatography using TALON resins (Takara, Japan) and stored in PBS buffer at 4 °C until AFM-SMFS experiments.

Constructs for proteins  $SNAP-(GB1)_2-SNAP$ ,  $SNAP-(GB1)_4-SNAP$ ,  $SNAP-(GB1)_8-SNAP$ ,  $SNAP-(GB1)_{16}-SNAP$ ,  $SNAP-(NuG2)_2-SNAP$ ,  $SNAP-(NuG2)_4-SNAP$ ,  $SNAP-(NuG2)_8-SNAP$ ,  $SNAP-(NuG2)_{16}-SNAP$ ,  $SNAP-SdrGB1-SNAP$ ,  $SNAP-(SdrGB1)_2-SNAP$ ,  $SNAP-(SdrGB1)_4-SNAP$  and  $SNAP-(SdrGB1)_8-SNAP$  were similarly cloned into pQE80L vectors, then expressed and purified as described above. These proteins were dialyzed into deionized water and lyophilized before use. All these constructs and full amino acid sequences are shown in Supplemental Material [25].

### 2. AFM sample preparation

More detailed AFM-based single-molecule force spectroscopy protocol has been described previously [23]. In brief, AFM cantilevers (Bruker, MLCT, USA) and glass substrates (Sail Brand, China) were hydroxylated by immersion in chromic acid at 80 °C for 30 min, following by aminosilanization in anhydrous toluene solution with 1% (v/v) APTES (Merck, USA) for 1 h. Then the cantilevers and substrates were rinsed with toluene, ethanol, and dried under nitrogen, incubated at 80 °C for 45 min, and stored under argon.

Prior to AFM-SMFS experiments, both glass substrates and cantilevers were functionalized with maleimide through incubation in DMSO with 0.2 mM Mal-PEG-NHS (MW: 5000 Da, Nanocs, USA) for 1 h, and then washed with DMSO, ethanol and dried with nitrogen

stream. Finally, the glass substrates and cantilevers were kept dry at  $-20\text{ }^\circ\text{C}$  before use.

### 3. AFM-based single-molecule force spectroscopy

All single-molecule force measurements were performed with a commercial AFM system (Bruker, NanoWizard IV, USA) in Tris buffer (pH 7.4) with or without EDTA (10 mM) at room temperature (25 °C). Silicon nitride MLCT-D cantilevers with spring constant of  $50\text{ pN nm}^{-1}$  were used and calibrated using the equipartition theorem for each measurement. During the measurement, the cantilever was briefly and gently ( $\sim 300\text{ pN}$ ) brought in contact with the glass surface and held for 0.5 s, then retracted at a constant speed of  $1\text{ }\mu\text{m s}^{-1}$ . The force-extension curves were recorded using JPK data processing software and further analyzed with a custom-written procedure in Igor 6.37 (Wavemetric Inc.).

### 4. Hydrogel preparation and mechanical test

To prepare the hydrogels, self-synthesized O6-benzylguanine styrene [18] was covalently conjugated to SNAP-protein-SNAP at a molar ratio of 2:1 in a shaker at 4 °C overnight. Then the solutions were mixed with acrylamide, LAP (0.05%) and transferred to 1 mm-thick custom-made transparent glass molds, and polymerized under UV illumination for 30 min at room temperature. Subsequently, the formed hydrogels were soaked in Tris buffer at 4 °C for 24 h to reach the equilibrium-swollen state. All hydrogel samples were in an identical geometry, with a length of 12, a width of 1.6, and a height of 15 mm. Tensile tests were performed using an Instron-5944 tensometer with a 10-N static load cell at room temperature. Fatigue experiments were performed in a humidity- and temperature-controlled environment using an integrated humidifier to minimize water evaporation from the hydrogel samples during long-term cyclic loading.

- 
- [1] X. Li and J. P. Gong, *Design principles for strong and tough hydrogels*, *Nat. Rev. Mater.* **9**, 380 (2024).
  - [2] X. Zhao, X. Chen, H. Yuk, S. Lin, X. Liu, and G. Parada, *Soft materials by design: Unconventional polymer networks give extreme properties*, *Chem. Rev.* **121**, 4309 (2021).
  - [3] Y. Lee, W. J. Song, and J. Y. Sun, *Hydrogel soft robotics*, *Mater. Today Phys.* **15**, 100258 (2020).
  - [4] J. Tang, J. Li, J. J. Vlassak, and Z. Suo, *Fatigue fracture of hydrogels*, *Extreme Mech. Lett.* **10**, 24 (2017).
  - [5] R. Bai, Q. Yang, J. Tang, X. P. Morelle, J. Vlassak, and Z. Suo, *Fatigue fracture of tough hydrogels*, *Extreme Mech. Lett.* **15**, 91 (2017).
  - [6] G. J. Lake and A. G. Thomas, *Strength of highly elastic materials*, *Proc. R. Soc. A* **300**, 108 (1967).
  - [7] S. Lin and X. Zhao, *Fracture of polymer networks with diverse topological defects*, *Phys. Rev. E* **102**, 052503 (2020).
  - [8] B. Deng, S. Wang, C. Hartquist, and X. Zhao, *Nonlocal intrinsic fracture energy of polymerlike networks*, *Phys. Rev. Lett.* **131**, 228102 (2023).

- [9] S. Wang, S. Panyukov, S.L. Craig, and M. Rubinstein, *Contribution of unbroken strands to the fracture of polymer networks*, *Macromolecules* **56**, 2309 (2023).
- [10] C.M. Hartquist, S. Wang, B. Deng, H.K. Beech, S.L. Craig, B.D. Olsen, M. Rubinstein, and X. Zhao, *Fracture of polymer-like networks with hybrid bond strengths*, *J. Mech. Phys. Solids* **195**, 105931 (2025).
- [11] Z. J. Wang, S. Wang, J. Jiang, Y. Hu, T. Nakajima, S. Maeda, S.L. Craig, and J.P. Gong, *Effect of the activation force of mechanophore on its activation selectivity and efficiency in polymer networks*, *J. Am. Chem. Soc.* **146**, 13336 (2024).
- [12] G.E. Sanoja, X.P. Morelle, J. Comtet, C.J. Yeh, M. Ciccotti, and C. Creton, *Why is mechanical fatigue different from toughness in elastomers? the role of damage by polymer chain scission*, *Sci. Adv.* **7**, eabg9410 (2021).
- [13] J.Z. Ju, G.E. Sanoja, L. Cipelletti, M. Ciccotti, B.G. Zhu, T. Narita, C.Y. Hui, and C. Creton, *Role of molecular damage in crack initiation mechanisms of tough elastomers*, *Proc. Natl. Acad. Sci. U.S.A.* **121**, e2410515121 (2024).
- [14] E. Ducrot, Y. Chen, M. Bulters, R.P. Sijbesma, and C. Creton, *Toughening elastomers with sacrificial bonds and watching them break*, *Science* **344**, 186 (2014).
- [15] J. Sloodman, V. Waltz, C.J. Yeh, C. Baumann, R. Gostl, J. Comtet, and C. Creton, *Quantifying rate- and temperature-dependent molecular damage in elastomer fracture*, *Phys. Rev. X* **10**, 041045 (2020).
- [16] J.Z. Ju, G.E. Sanoja, M.Y. Nagazi, L. Cipelletti, Z.Z. Liu, C.Y. Hui, M. Ciccotti, T. Narita, and C. Creton, *Real-time early detection of crack propagation precursors in delayed fracture of soft elastomers*, *Phys. Rev. X* **13**, 021030 (2023).
- [17] S. Wang, H.K. Beech, B.H. Bowser, T.B. Kouznetsova, B.D. Olsen, M. Rubinstein, and S.L. Craig, *Mechanism dictates mechanics: A molecular substituent effect in the macroscopic fracture of a covalent polymer network*, *J. Am. Chem. Soc.* **143**, 3714 (2021).
- [18] H. Lei *et al.*, *Stretchable hydrogels with low hysteresis and anti-fatigue fracture based on polyprotein cross-linkers*, *Nat. Commun.* **11**, 4032 (2020).
- [19] K.C. Neuman and A. Nagy, *Single-molecule force spectroscopy: Optical tweezers, magnetic tweezers and atomic force microscopy*, *Nat. Method* **5**, 491 (2008).
- [20] H. Lei, C. He, C. Hu, J. Li, X. Hu, X. Hu, and H. Li, *Single-molecule force spectroscopy trajectories of a single protein and its polyproteins are equivalent: A direct experimental validation based on a small protein NuG<sub>2</sub>*, *Angew. Chem., Int. Ed.* **56**, 6117 (2017).
- [21] Y. Cao and H. Li, *Polyprotein of Gb1 is an ideal artificial elastomeric protein*, *Nat. Mater.* **6**, 109 (2007).
- [22] L.F. Milles, E.M. Unterauer, T. Nicolaus, and H.E. Gaub, *Calcium stabilizes the strongest protein fold*, *Nat. Commun.* **9**, 4764 (2018).
- [23] H. Lei, Q. Ma, W. Li, J. Wen, H. Ma, M. Qin, W. Wang, and Y. Cao, *An ester bond underlies the mechanical strength of a pathogen surface protein*, *Nat. Commun.* **12**, 5082 (2021).
- [24] O.K. Dudko, G. Hummer, and A. Szabo, *Theory, analysis, and interpretation of single-molecule force spectroscopy experiments*, *Proc. Natl. Acad. Sci. U.S.A.* **105**, 15755 (2008).
- [25] See Supplemental Material at <http://link.aps.org/supplemental/10.1103/bcq4-xw5q> for relevant details of the experiment and theoretical model. It includes the amino acid sequences of all protein domains used in our system, the SDS-PAGE gel image, fatigue fracture tests for all gels, the theoretical model in detail, and the parameters used for the simulation.
- [26] E.E. Gdoutos, *Fracture Mechanics, Solid Mechanics and Its Applications* (Springer, Cham, 2020), Vol. 263.
- [27] J.R. Rice, *A path independent integral and approximate analysis of strain concentration by notches and cracks*, *J. Appl. Mech.* **35**, 379 (1968).
- [28] G.I. Bell, *Models for specific adhesion of cells to cells*, *Science* **200**, 618 (1978).
- [29] J.R. Rice and G.F. Rosengren, *Plane strain deformation near a crack tip in a power-law hardening material*, *J. Mech. Phys. Solids* **16**, 1 (1968).
- [30] J.W. Hutchinson, *Singular behaviour at end of a tensile crack in a hardening material*, *J. Mech. Phys. Solids* **16**, 13 (1968).
- [31] S. Wang, Y. Hu, T.B. Kouznetsova, L. Sapir, D. Chen, A. Herzog-Arbeitman, J.A. Johnson, M. Rubinstein, and S.L. Craig, *Facile mechanochemical cycloreversion of polymer cross-linkers enhances tear resistance*, *Science* **380**, 1248 (2023).
- [32] C. Hartquist, S. Wang, Q.D. Cui, W. Matusik, B.L. Deng, and X.H. Zhao, *Scaling law for intrinsic fracture energy of diverse stretchable networks*, *Phys. Rev. X* **15**, 011002 (2025).
- [33] S.T. Lin, J.H. Ni, D.C. Zheng, and X.H. Zhao, *Fracture and fatigue of ideal polymer networks*, *Extreme Mech. Lett.* **48**, 101399 (2021).
- [34] Z. Wang *et al.*, *Toughening hydrogels through force-triggered chemical reactions that lengthen polymer strands*, *Science* **374**, 193 (2021).
- [35] Z.J. Wang, W. Li, X. Li, T. Nakajima, M. Rubinstein, and J.P. Gong, *Rapid self-strengthening in double-network hydrogels triggered by bond scission*, *Nat. Mater.* **24**, 607 (2025).
- [36] M. Hua *et al.*, *Strong tough hydrogels via the synergy of freeze-casting and salting out*, *Nature (London)* **590**, 594 (2021).
- [37] X. Liang *et al.*, *Anisotropically fatigue-resistant hydrogels*, *Adv. Mater.* **33**, 2102011 (2021).
- [38] S. Lin, J. Liu, X. Liu, and X. Zhao, *Muscle-like fatigue-resistant hydrogels by mechanical training*, *Proc. Natl. Acad. Sci. U.S.A.* **116**, 10244 (2019).
- [39] H. Yang, X. Chen, B.A. Sun, J.D. Tang, and J.J. Vlassak, *Fracture tolerance induced by dynamic bonds in hydrogels*, *J. Mech. Phys. Solids* **169**, 105083 (2022).
- [40] Y.H. Xiao, Q. Li, X. Yao, R.B. Bai, W. Hong, and C.H. Yang, *Fatigue of amorphous hydrogels with dynamic covalent bonds*, *Extreme Mech. Lett.* **53**, 101679 (2022).
- [41] X. Li and J.P. Gong, *Role of dynamic bonds on fatigue threshold of tough hydrogels*, *Proc. Natl. Acad. Sci. U.S.A.* **119**, e2200678119 (2022).
- [42] J. Kim, G. Zhang, M. Shi, and Z. Suo, *Fracture, fatigue, and friction of polymers in which entanglements greatly outnumber cross-links*, *Science* **374**, 212 (2021).